Supporting Information for

Structures of the peptide-modifying radical SAM enzyme SuiB elucidate the basis of substrate recognition

Katherine M. Davis[1], Kelsey R. Schramma[1], William A. Hansen[2], John P. Bacik[1], Sagar D. Khare[2], Mohammad R. Seyedsayamdost[1,3], Nozomi Ando[1]**

Departments of Chemistry[1] and Molecular Biology[3], Princeton University, Princeton, New Jersey 08544, USA.

Department of Chemistry and Chemical Biology[2], Rutgers University, New Brunswick, New Jersey 08901, USA.

* To whom correspondence should be addressed.

Phone: 609-258-5941, E-mail: mrseyed@princeton.edu

Phone: 609-258-6513, E-mail: nozomi.ando@princeton.edu

SI RESULTS/ANALYSIS

SAM binding and the Active Site

Hydrogen bond stabilization of the various SAM moieties is critical for positioning the co-substrate about the cluster (Fig. S1). Related hydrogen-bonding motifs include the "GGE" motif, important for methionine orientation; the ribose motif; as well as the "GXIXGXXE" motif and β6 or "adenine binding" motif, both involved in stabilizing the adenine moiety (1-3). Interactions with the adenine component include hydrogen bonds to the Ser279 backbone of the β6 strand, the Phe123 carbonyl group, as well as hydrophobic interactions with Val249. Likewise, side chains of Ser210 and Asn247, residues in the ribose and GXIXGXXE motifs respectively, help to position the ribose moiety by providing hydrogen-bonding partners for the 3'-hydroxyl group. It is clear from the higher resolution post-cleavage structure that Gln212 also indirectly contributes to ribose stabilization through a water-mediated hydrogen bond. In contrast, proper arrangement of methionine is primarily provided by hydrogen bonds with the GGE motif, following the β2 strand. To facilitate bonding, the carbonyl group of the second glycine points toward methionine, making it a rare cis-isomer. While common to many radical SAMs, this Gly160-Met interaction is supplemented by additional hydrogen bonding with the Glu161 side chain.

Evaluation of large-scale movements upon substrate binding

An examination of the post SAM-cleavage structure reveals significant conformational changes in both the radical SAM and RRE domains (Fig. S6A). Although minimal interactions are observed between SuiA and the RRE in SuiB, calculations comparing the N-terminal domains yield a Cα RMSD of 1.85 Å or 3.97 Å for chains A and B respectively, in contrast to an average of only 0.294 ± 0.011 Å upon SAM binding (Fig. 4A). The wHTH domain, in particular, appears to angle outward away from the mouth of the barrel. The intensity of this effect is chain dependent, as is the involvement of $\alpha 4_n$ (Fig. 4A and S6A).

Additional helix links wHTH domain to the catalytic barrel

An analogous helix to α4n has been observed in the microcin C biosynthetic enzyme MccB for which the RRE serves as a peptide clamp (4). Structurally, this helix follows consecutively from the wHTH domain in SuiB, while the MccB homodimer utilizes a domain-swapping mechanism

to generate a similar motif. In both enzymes, the ancillary helix (Fig. S3, grey) forms significant van der Waals and hydrophobic interactions with the primary helix, α1, of the adjacent bundle at an approximate crossing angle of 50°. Although direct comparisons are difficult given the precursor peptide of MccB lacks a leader sequence, this additional helix may play a structural role in orienting the RRE with respect to the catalytic core. Unfortunately, without peptide bound to the RRE, it is unclear whether it is required for peptide binding, or simply serves as a stabilizing link to the catalytic domain.

SI MATERIALS AND METHODS

Materials and Strains

The genomic DNA of *Streptococcus suis* 92-4172 was kindly provided by Prof. Marcelo Gottschalk at the University of Montreal, Canada. SuiB was cloned as a hexa-His-tagged construct, purified, reconstituted, and pre-reduced with sodium dithionite as recently reported (5). Reconstituted SuiB contained 10.4 ± 0.1 Fe and 9.0 ± 0.1 S per protomer. SuiA was synthesized and purified as described (5). Its identity was verified by high-resolution (HR) HPLC-MS ($[M+2H]^{2+}_{calc}$ 1216.6016 $[M+2H]^{2+}_{obs}$ 1216.60301, Δppm~1.2). Wt, reconstituted SuiB turned over substrate SuiA with a $V_{max}/[E]_T$ of 0.18 min^{-1}.

Crystallization

Crystals of N-terminally His_6-tagged SuiB were grown anaerobically in a glove box (Coy Laboratory Products) under a 97% N_2, 3% H_2 atmosphere using the sitting well vapor diffusion method. Crystallization trays were chilled on a cold block (~4 °C) during preparation, and all solutions were incubated at 12°C (Torrey Pines Scientific Incubator) prior to mixing to minimize nucleation events. All trays were incubated and maintained at 12°C during growth and storage.

To obtain the SuiA-bound structure, a solution containing 23 mg/mL of His_6-tagged SuiB in storage buffer [100 mM HEPES, pH 7.5, 300 mM KCl, 5 mM DTT, 10% (v/v) glycerol] was mixed with a stock solution of SuiA in storage buffer lacking DTT, yielding a final SuiA concentration of 1.9 mM. The resulting solution was incubated at 12°C for 10 min after which it was combined 1:1 with precipitant solution to form a 4 µL drop. The precipitant solution was generated by combining 100 mM Bis-Tris, pH 6.0, 200 mM LiS_2SO_4, 27% (w/v) PEG 3350 with 210 mM SAM in water to yield a final SAM concentration of 10.5 mM. Crystals appeared within 2 days and were fully formed (~75 x 75 μm^2) within a week. Sheet-like crystals were gently separated, looped and transferred briefly into cryoprotectant [200 mM Li_2SO_4, 53.8 mM BIS-TRIS, 27% (w/v) PEG 3350, 26% (v/v) PEG 400, 6 mM SAM] before cryocooling in liquid nitrogen.

To obtain the apo and SAM-bound structures, a solution containing 18.9 mg/mL His_6-tagged SuiB was mixed 1:1 with precipitant solution to generate a final drop volume of 4 µL. Numerous small (< 50 µm) star-like clusters of flat rod-shaped crystals were formed within 24 hrs. A seed stock was then produced by combining a single sitting well with 10 µL of reservoir

solution and 10 μL of SuiB at 8 mg/mL, followed by brief vortexing. Seed stock dilutions up to 10^7 were made with the same 1:1 protein/reservoir solution. Crystals were harvested from the $10^6/10^7$ dilutions drops approximately 2 days following seeding. The precipitant solution was 100 mM MES, pH 6.0, 15% (w/v) PEG 3350; cryoprotection was achieved by brief sequential transfer between precipitant solutions with increasing glycerol concentrations of 5%, 10% and 30% (v/v).

To obtain the structure with SAM, crystals of SuiB were incubated in precipitant solution containing ~6 mM SAM for 30 min prior to brief sequential transfer between precipitant solutions containing 6 mM SAM and increasing glycerol concentrations of 5%, 10% and 30% (v/v) glycerol. Although spontaneous cleavage of SAM has been observed in the homologous protein StrB and other radical SAM enzymes (1,6), given excess SAM in the soaking condition, a single abortive cleavage event would result in oxidation of the cluster, preventing further activity of the enzyme and yielding intact SAM in the active site.

Crystallographic Data Collection and Processing

All data were indexed, integrated and scaled using XDS software followed by merging with AIMLESS (7,8). Model building was completed in COOT (9) and subsequent refinements/calculations were performed in Phenix (10). Model quality was assessed using Molprobity (11). Data processing and refinement statics can be found in Table S1. Figures depicting the structure were generated with PyMol.

Phasing and Model Building. Single wavelength Fe-anomalous diffraction was collected for a crystal in the absence of substrate at beamline 23-ID-B of the Advanced Photon Source (APS) at Argonne National Laboratory (Chicago, IL) on a MARmosaic 300 CCD detector. The crystal was maintained at 100 K and data were collected using inverse beam ($\Delta\phi = 1°$, wedge = 30°) at the Fe peak (λ, 1.7369 Å). Diffraction approached 2.93 Å with anomalous signal extending to 4.0 Å. Experimental phases were generated with the AutoSol Wizard (12). The hybrid substructure search submodule, HySS, yielded twenty-four heavy atom sites with a figure of merit of 0.39 through 4.0 Å. This is consistent with the presence of three [4Fe-4S] clusters in each of the two asymmetric copies. Solvent flattening was performed with RESOLVE, and the density-modified output map was used to manually generate a basic structure. This model was further augmented using rigid body refinement on a native dataset (λ, 0.6299 Å) from a different

crystal collected sequentially ($\Delta\phi$ = 0.25°) at the Cornell High Energy Synchrotron Source (CHESS), beamline A1 on a Pilatus 6M (Dectris) detector. The initial model contained two molecules in the asymmetric unit.

For structures solved in the absence of peptide substrate (SuiA), higher resolution native datasets (λ, 1.0332 Å) were obtained at 23-ID-D at the Advanced Photon Source (APS). Data were collected sequentially ($\Delta\phi$ = 0.1 – 0.2°) at 100 K with the Pilatus 6M (Dectris) detector. Structures of the substrate-free, and SAM-bound enzyme were solved using rigid body refinement of the initial model to 2.5 Å. In each of these structures, there are two molecules in the asymmetric unit; residues that were not modeled due to disorder are listed in Table S2. Note that the structure of the substrate-free enzyme includes an additional residue at the N-terminus of chain B. The structure of the SAM-bound enzyme includes an intact SAM molecule in each chain. Three [4Fe-4S] clusters were built into each chain of the structures. B-factors near the radical SAM cluster in chain B are consistently higher than the average for the structure.

Co-crystallization with SuiA/SAM. A native dataset for reconstituted enzyme co-crystallized with SAM and SuiA was also collected at the APS on the 23-ID-B setup described above. Data were collected sequentially ($\Delta\phi$ = 1°) at a wavelength of 1.033 Å. The structure was solved via molecular replacement with the initial enzyme model to yield a 2.1 Å structure with one molecule in the asymmetric unit. The main chain is complete, with methionine and SAM bound in the active site. The substrate peptide, SuiA, is bound, but electron density for residues -14 and 1 to 8 was insufficient to enable building.

Computational Methods

Four separate simulations were used to investigate the energy landscapes of the modeled core peptide within the determined SuiB crystal structure. In each simulation, we produced an ensemble of spatial starting orientations for the core peptide fragment, whose internal structure was modeled using molecular dynamics constrained by NMR structure-derived constraints (5,7), connected to the leader peptide in the SuiB crystal structure active site. In the first two simulations, referred to as SAMsim_cycle and SAMsim_linear, we sampled the core peptide in the presence of an intact SAM found within the solved crystal structure with (cycle) and without (linear) a covalent bond constraint between Lys2 (Cβ) and Trp6 (Cζ2) respectively. The second set of two simulations, 5ADsim_cycle and 5ADsim_linear, were performed in the presence of

the cleaved SAM product 5'-deoxyadenosine (5AD) also with and without a Lys-Trp covalent bond present. All 5ADsim simulations were performed with an additional distance constraint added between the core peptide Lys (Cβ) and the 5'-deoxyadenosine 5'C atom (d = 2.8-4.3 Å). The simulations had the following three steps:

1) Appending the core peptide with Rosetta Match and Kinematic Loop Closure

Rosetta Match (13) was used to locate geometrically compatible positions of the core peptide. First, we created a ligand model of the NMR-derived core peptide structure. The ligand model was comprised of the Cα atoms of the core peptide structure. Using Rosetta Match and a set of geometric constraints derived from a non-redundant set of high-resolution protein structures (nr database), we located all possible core-peptide Cα ligand model placements within the solved crystal structure active site. The ligand model placements positioned the core peptide in a sterically favorable position while maintaining chain connectivity with the leader peptide. To obtain these placements, we applied geometric matching constraints between the C-terminal Cα atoms of the leader peptide and N-terminal Cα atoms of the core peptide Cα ligand model. These geometric constraints were obtained from measuring distance and angle values of contiguous sets of Cα atoms within heptapeptide fragments in the nr database. Using these constraints in Rosetta Match, we produced 1296 core peptide placements that did not sterically clash with the SuiB scaffold backbone. For each compatible placement, we converted the Cα ligand model to an all-atom model and generated a contiguous peptide chain using a generalized kinematic loop closure (genKIC) protocol (14). The genKIC protocol produced 468 starting structures in which the peptide bond geometries at the connection point were ideal.

2) Sampling core peptide conformations within a poly-alanine active site

In order to enhance the efficiency of conformational space sampling by the core peptide, structures obtained in step 1 were subjected to four cycles of Rosetta FastRelax (15) within a poly-alanine model of the active site using a scoring function that emphasizes the repulsive component of the Lennard Jones potential (16). Residues whose Cα atoms were within 8 Å of the core peptide Cα atoms were converted to alanine before this step and subsequently returned to their native sidechain conformations after FastRelax. While sampling, we placed NMR derived pseudo-covalent geometry constraints (5,17) between the core peptide residues Lys2 and

Trp6, which are involved in the crosslinking reaction, to maintain this covalent linkage. Both the core peptide sidechain and backbone degrees of freedom were sampled. Coordinate constraints were placed on all remaining residues (leader peptide and SuiB-scaffold) to prevent their movement during the simulation. At the end of FastRelax, a final round of rotameric sampling of the core peptide followed by energy minimization (18) was applied with a fixed backbone.

3) Refinement of core peptide within the native active site

We next applied a second round of FastRelax (four cycles), rotameric sampling (four cycles) followed by energy minimization on the conformations generated in step 2. For SAMsim_cycle and SAMsim_liner we maintained the crystal structure sidechain conformations in the leader-peptide and the SuiB-scaffold by placing coordinate constraints on all crystal-structure residues during the FastRelax and rotameric-sampling stages. Additionally, only the core peptide was allowed to sample both rotameric and backbone degrees of freedom. For 5ADsim_cycle and 5ADsim_linear, we performed simulations with and without rotameric sampling of 11 active-site residues (24, 26, 108, 110, 158, 245, 247, 272, 315, 319, and 355). The pseudo-covalent and coordinate constraints from step 2 were maintained in step 3 for SAMsim_cycle and 5ADsim_cycle. Additionally, in the 5ADsim_cycle and 5ADsim_linear, a second distance constraint of 3.5 Å was placed between the 5'-carbon of 5'-deoxyadenosine and the beta-carbon of Lys2 in the core peptide.

All Rosetta scripts and geometric constraint blocks used in the Rosetta simulation are provided below:

1. Matcher constraint block used to locate geometrically compatible conformations of the core peptide with respect to the leader peptide as described in Step 1

```
CST::BEGIN
  TEMPLATE::  ATOM_MAP: 1 atom_name: C1 C2 C3
  TEMPLATE::  ATOM_MAP: 1 residue3: SUI

  TEMPLATE::  ATOM_MAP: 2 atom_name: C CA N
  TEMPLATE::  ATOM_MAP: 2 is_backbone
  TEMPLATE::  ATOM_MAP: 2 residue3: ALA

  CONSTRAINT::  distanceAB: 5.1147    1.036 10.0   0       1
  CONSTRAINT::     angle_A: 111.774   53.71 10.0   360.0   3
  CONSTRAINT::     angle_B: 134.685  25.928 10.0   360.0   3
  CONSTRAINT::   torsion_A: 0.00      180.0 10.0   360.0   12
  CONSTRAINT::   torsion_B: 0.00      180.0 10.0   360.0   12
  CONSTRAINT::  torsion_AB: 0.00      180.0 10.0   360.0   12
  ALGORITHM_INFO:: match
    IGNORE_UPSTREAM_PROTON_CHI
  ALGORITHM_INFO::END
```

```
CST::END

CST::BEGIN
  TEMPLATE::  ATOM_MAP: 1 atom_name: C1 C2 C3
  TEMPLATE::  ATOM_MAP: 1 residue3: SUI

  TEMPLATE::  ATOM_MAP: 2 atom_name: C CA N
  TEMPLATE::  ATOM_MAP: 2 is_backbone
  TEMPLATE::  ATOM_MAP: 2 residue3: SER

  CONSTRAINT::  distanceAB: 6.875     2.875 10.0   0       1
  CONSTRAINT::     angle_A: 105.00    55.00 10.0   360.0   4
  CONSTRAINT::     angle_B: 125.00    45.00 10.0   360.0   4
  CONSTRAINT::   torsion_A: 0.00      180.0 10.0   360.0   12
  CONSTRAINT::   torsion_B: 0.00      180.0 10.0   360.0   12
  CONSTRAINT::  torsion_AB: 0.00      180.0 10.0   360.0   12
  ALGORITHM_INFO:: match
    IGNORE_UPSTREAM_PROTON_CHI
  ALGORITHM_INFO::END
CST::END

CST::BEGIN
  TEMPLATE::  ATOM_MAP: 1 atom_name: C1 C2 C3
  TEMPLATE::  ATOM_MAP: 1 residue3: SUI

  TEMPLATE::  ATOM_MAP: 2 atom_name: C CA N
  TEMPLATE::  ATOM_MAP: 2 is_backbone
  TEMPLATE::  ATOM_MAP: 2 residue3: SER

  CONSTRAINT::  distanceAB: 8.5       4.5   10.0   0       1
  CONSTRAINT::     angle_A: 110.0      70.0 10.0   360.0   5
  CONSTRAINT::     angle_B: 120.0      60.0 10.0   360.0   5
  CONSTRAINT::   torsion_A: 0.00      180.0 10.0   360.0   12
  CONSTRAINT::   torsion_B: 0.00      180.0 10.0   360.0   12
  CONSTRAINT::  torsion_AB: 0.00      180.0 10.0   360.0   12
  ALGORITHM_INFO:: match
    IGNORE_UPSTREAM_PROTON_CHI
  ALGORITHM_INFO::END
CST::END
```

2. Generalized kinematic loop closure xml code block used in step 1

```
ROSETTASCRIPTS>
        <SCOREFXNS>
                <bb_hbond_tors_fadun_cst weights="empty.wts" symmetric=0>
                        <Reweight scoretype=hbond_sr_bb weight=1.17 />
                        <Reweight scoretype=hbond_lr_bb weight=1.17 />
                        <Reweight scoretype=omega weight=0.5 />
                        <Reweight scoretype=rama weight=0.2 />
                        <Reweight scoretype=p_aa_pp weight=0.32 />
                        <Reweight scoretype=coordinate_constraint weight=10.0 />
                        <Reweight scoretype=atom_pair_constraint weight=1.0 />
                        <Reweight scoretype=angle_constraint weight=1.0 />
                        <Reweight scoretype=dihedral_constraint weight=1.0 />
                </bb_hbond_tors_fadun_cst>
        </SCOREFXNS>
        <RESIDUE_SELECTORS>
                <Index name=loop resnums=%%loop_range%% />
                <Not name=not_loop selector=loop />
        </RESIDUE_SELECTORS>
        <TASKOPERATIONS>
                <InitializeFromCommandline name=init/>
                <IncludeCurrent name=keep_curr/>
                <OperateOnResidueSubset name=nodesrep_notloop selector=loop >
                        <PreventRepackingRLT/>
                </OperateOnResidueSubset>
                <OperateOnResidueSubset name=nodes_loop selector=not_loop >
                        <RestrictToRepackingRLT/>
                </OperateOnResidueSubset>
        </TASKOPERATIONS>
        <FILTERS>
                <ContingentFilter name=kicedA_B />
        </FILTERS>
        <MOVERS>
                <DeclareBond name=bond1 res1=%%one%% atom1="C" res2=%%two%% atom2="N"/>
                <GeneralizedKIC name="genkic" closure_attempts=800 stop_if_no_solution=0 stop_when_n_solutions_found=100
selector="lowest_energy_selector" selector_scorefunction="bb_hbond_tors_fadun_cst" selector_kbt=1.0 contingent_filter="kicedA_B">
                        <AddResidue res_index=%%one%% />
                        <AddResidue res_index=%%two%% />
                        <AddResidue res_index=%%three%% />
                        <SetPivots res1=%%one%% atom1="CA" res2=%%two%% atom2="CA" res3=%%three%% atom3="CA" />
                        <CloseBond prioratom_res=%%one%% prioratom="CA" res1=%%one%% atom1="C" res2=%%two%% atom2="N"
followingatom_res=%%two%% followingatom="CA" bondlength=1.325 angle1=120 angle2=120 randomize_flanking_torsions=true />
                        <AddPerturber effect="randomize_alpha_backbone_by_rama">
                                <AddResidue index=%%one%% />
                                <AddResidue index=%%two%% />
                                <AddResidue index=%%three%% />
                        </AddPerturber>
                        <AddPerturber effect="set_dihedral">
```

```
                                                <AddAtoms res1=%%one%% atom1="CA" res2=%%one%% atom2="C" res3=%%two%% atom3="N" res4=%%two%%
    atom4="CA"/>
                                                <AddValue value=180.0/>
                                        </AddPerturber>
                                        <AddFilter type="loop_bump_check"/>
                                </GeneralizedKIC>
                                <AtomCoordinateCstMover name=loopsCST coord_dev=0.2  bounded=true bound_width=0.1 sidechain=true native=false
    task_operations=nodes_loop />
            </MOVERS>
            <PROTOCOLS>
                                <Add mover=bond1/>
                                <Add mover=loopsCST/>
                                <Add mover=genkic/>
                                <Add filter=kicedA_B/>
            </PROTOCOLS>
    </ROSETTASCRIPTS>
```

3. Enzdes constraint block used to place constraints between Lys2 and Trp6 in the core peptide as well as between core peptide and 5□-deoxyadenosine. (Steps 2 and 3)

```
CST::BEGIN
  TEMPLATE::  ATOM_MAP: 1 atom_name: CB CA N
  TEMPLATE::  ATOM_MAP: 1 residue3: LYS

  TEMPLATE::  ATOM_MAP: 2 atom_name: CZ2 CE2 NE1
  TEMPLATE::  ATOM_MAP: 2 is_backbone
  TEMPLATE::  ATOM_MAP: 2 residue3: TRP

  CONSTRAINT::  distanceAB: 1.551     0.030 1000.0   1
  CONSTRAINT::     angle_A: 104.927   5.00  100.0   360.0
  CONSTRAINT::     angle_B: 119.682   5.00  100.0   360.0
  CONSTRAINT::   torsion_A: 179.689   20.00 10.0   360.0
  CONSTRAINT::   torsion_B: 0.813     20.00 10.0   360.0
  CONSTRAINT::  torsion_AB: 70.909    20.00 10.0   360.0
CST::END

CST::BEGIN
  TEMPLATE::  ATOM_MAP: 1 atom_name: CB CA N
  TEMPLATE::  ATOM_MAP: 1 residue3: LYS

  TEMPLATE::  ATOM_MAP: 2 atom_name: C10 C8 N9
  TEMPLATE::  ATOM_MAP: 2 residue3: 5AD

  CONSTRAINT::  distanceAB: 3.500     0.60 100.0   1
CST::END
```

4. XML code block used to run steps 2 and 3 in computational methods

```
<ROSETTASCRIPTS>
  <SCOREFXNS>
      <scorefxn1 weights=talaris2013_cst >
            <Reweight scoretype=atom_pair_constraint weight=1.0 />
            <Reweight scoretype=angle_constraint weight=1.0 />
            <Reweight scoretype=dihedral_constraint weight=1.0 />
            <Reweight scoretype=coordinate_constraint weight=1.0 />
            Reweight scoretype=fa_rep weight=0.1 />
    </scorefxn1>
    <scorefxn2 weights=enzdes_polyA_min.wts />
  </SCOREFXNS?
  <RESIDUE_SELECTORS>
    <Index name=streptide resnums=457-465 />
    <Not name=atoms_with_density selector=streptide />
    <Index name=pocket_to_ala resnums=108,110,112,115,125,126,154,156,158,183,185,208,245,247,249,272,274,277,279,281,282,285,319,348,353,355,357,366,369 />
    <Not name=non_pocket_res selector=pocket_to_ala />
  </RESIDUE_SELECTORS>
  <TASKOPERATIONS>
            <InitializeFromCommandline name=init/>
            <IncludeCurrent name=keep_curr/>
    <OperateOnResidueSubset name=csts_for_non_streptide selector=streptide >
      <PreventRepackingRLT/>
    </OperateOnResidueSubset>
    <OperateOnResidueSubset name=repack_streptide selector=streptide >
      <RestrictToRepackingRLT/>
    </OperateOnResidueSubset>
    <OperateOnResidueSubset name=no_repack selector=atoms_with_density >
      <PreventRepackingRLT/>
    </OperateOnResidueSubset>
    <OperateOnResidueSubset name=pocket_to_ala selector=non_pocket_res >
      <PreventRepackingRLT/>
    </OperateOnResidueSubset>
  </TASKOPERATIONS>

  <FILTERS>
    <PoseInfo name=p_info />
```

```
    <ScoreType name=atom_pair_cst scorefxn=scorefxn1 score_type=atom_pair_constraint threshold=50 />
    <ScoreType name=ang_cst scorefxn=scorefxn1 score_type=angle_constraint threshold=50 />
    <ScoreType name=dihedral_cst scorefxn=scorefxn1 score_type=dihedral_constraint threshold=50 />
    <ScoreType name=coord_cst scorefxn=scorefxn1 score_type=coordinate_constraint threshold=10 />
    </FILTERS>

  <MOVERS>
    <AddOrRemoveMatchCsts name=enzCST cst_instruction="add_new" cstfile="trp_lys.cst" keep_covalent=1 />
    ConstraintSetMover name=cstADD add_constraints=true cst_file="all_heavy_atom.cst" />
    <AtomCoordinateCstMover name=poseCST coord_dev=0.002 bounded=true bound_width=0.1 sidechain=true native=false task_operations=csts_for_non_streptide />
    <AtomCoordinateCstMover name=streptide_bbCST coord_dev=0.6 bounded=true bound_width=0.3 sidechain=false native=false task_operations=repack_streptide />
    <MakePolyX name=convert_shell_to_ala keep_gly=1 task_operations=pocket_to_ala/>
    <SaveAndRetrieveSidechains name=rep_sidechains allsc=1 two_step=1 multi_use=1 jumpid=0/>
    <PackRotamersMover name=repack scorefxn=scorefxn1 task_operations=init,keep_curr,no_repack,repack_streptide/>
    <MinMover name=min scorefxn=scorefxn1 chi=1 bb=1 jump=0 cartesian=0 type=lbfgs_armijo_nonmonotone tolerance=0.001 max_iter=200/>

    <FastRelax name=fastrelax repeats=4 scorefxn=scorefxn2 task_operations=keep_curr,init,csts_for_non_streptide >
      <MoveMap>
        <Span begin=457 end=459 chi=1 bb=1/>
        <Span begin=460 end=465 chi=1 bb=0/>
      </MoveMap>
    </FastRelax>
    <LoopOver name=min_twice mover_name=min iterations=1 drift=true/>
    <ParsedProtocol name=repack_minimize>
              <Add mover=repack/>
              <Add mover=min/>
    </ParsedProtocol>
    <GenericMonteCarlo name=genericMC mover_name=repack_minimize scorefxn_name=scorefxn1 temperature=0.8 trials=4/>
  </MOVERS>
  <PROTOCOLS>
            Add mover=cstADD/>
    <Add mover=poseCST/>
    <Add mover=streptide_bbCST/>
    <Add mover=enzCST/>

    Add mover=rep_sidechains/>
    Add mover=convert_shell_to_ala/>
    Add mover=fastrelax/>
    Add mover=rep_sidechains/>
    Add mover=fastrelax/>

    Add filter=p_info/>
    Add filter=coord_cst/>

     <Add mover=genericMC/>
    Add filter=p_info/>
    Add filter=atom_pair_cst/>
    Add filter=ang_cst/>
    Add filter=dihedral_cst/>
    Add filter=coord_cst/>
  </PROTOCOLS>

</ROSETTASCRIPTS>
```

Table S1. Crystallographic data processing and refinement statistics for SuiB structures.

PDB ID (ligand)	5V1Q	5V1S (SAM)	5V1T (MET/SAM/SuiA)
Data Collection[a]			
Space group	$P2_12_12$	$P2_12_12$	$P2_12_12$
Unit cell (Å)	a = 115.23, b = 84.42, c = 110.04 $\alpha = \beta = \gamma = 90$	a = 114.79, b = 85.47, c = 109.86 $\alpha = \beta = \gamma = 90$	a = 69.37, b = 115.04, c = 54.33 $\alpha = \beta = \gamma = 90$
Wavelength (Å)	1.0332	1.0332	1.0332
Resolution range (Å)	29.51 – 2.50 (2.60 – 2.50)	29.47 – 2.49 (2.59 – 2.49)	29.24 – 2.10 (2.16 – 2.10)
Total observations	486901	248251	87295
Total unique observations	37704	38407	25903
I/σ_I	17.7 (1.9)	17.7 (2.0)	9.3 (1.9)
Completeness (%)	99.3 (94.4)	99.8 (99.0)	99.3 (97.1)
R_{merge}	0.096 (1.29)	0.067 (0.839)	0.123 (0.799)
R_{pim}	0.028 (0.395)	0.029 (0.373)	0.078 (0.502)
Redundancy	12.9 (11.5)	6.5 (5.9)	3.4 (3.4)
Refinement Statistics			
Resolution range (Å)	29.51 – 2.50	29.47 – 2.49	29.24 – 2.10
Reflections (total)	37648	38359	25862
Reflections (test)	1781	1714	2591
Total atoms refined	6778	6766	3971
Solvent	5	7	283
R_{work} (R_{free})	21.66 (25.68)	21.48 (26.97)	18.92 (22.27)
RMSDs			
Bond lengths (Å)/ angles (°)	0.005/0.659	0.008/0.799	0.006/0.942
Ramachandran plot			
Favored/allowed (%)	96.16/3.84	95.24/4.76	96.88/3.12
Mean B values (Å^2)			
Protein Chains A/B	79.65/79.11	74.36/72.95	31.84/--
[4Fe4S]/SAM/MET/SuiA	66.30/--/--/--	66.80/71.40/--/--	25.00/31.70/26.70/36.79
Solvent	71.27	65.40	35.94

[a] Values in parentheses refer to the high-resolution shell.

Table S2. Missing residues for each structure.

Missing Residues	**5V1Q**	**5V1S**	**5V1T**
Chain A	1, 75-81, 131-133	1, 74-81, 331-335	none
Chain B	none	127-132, 281-286	SuiA(-14), SuiA(1-8)

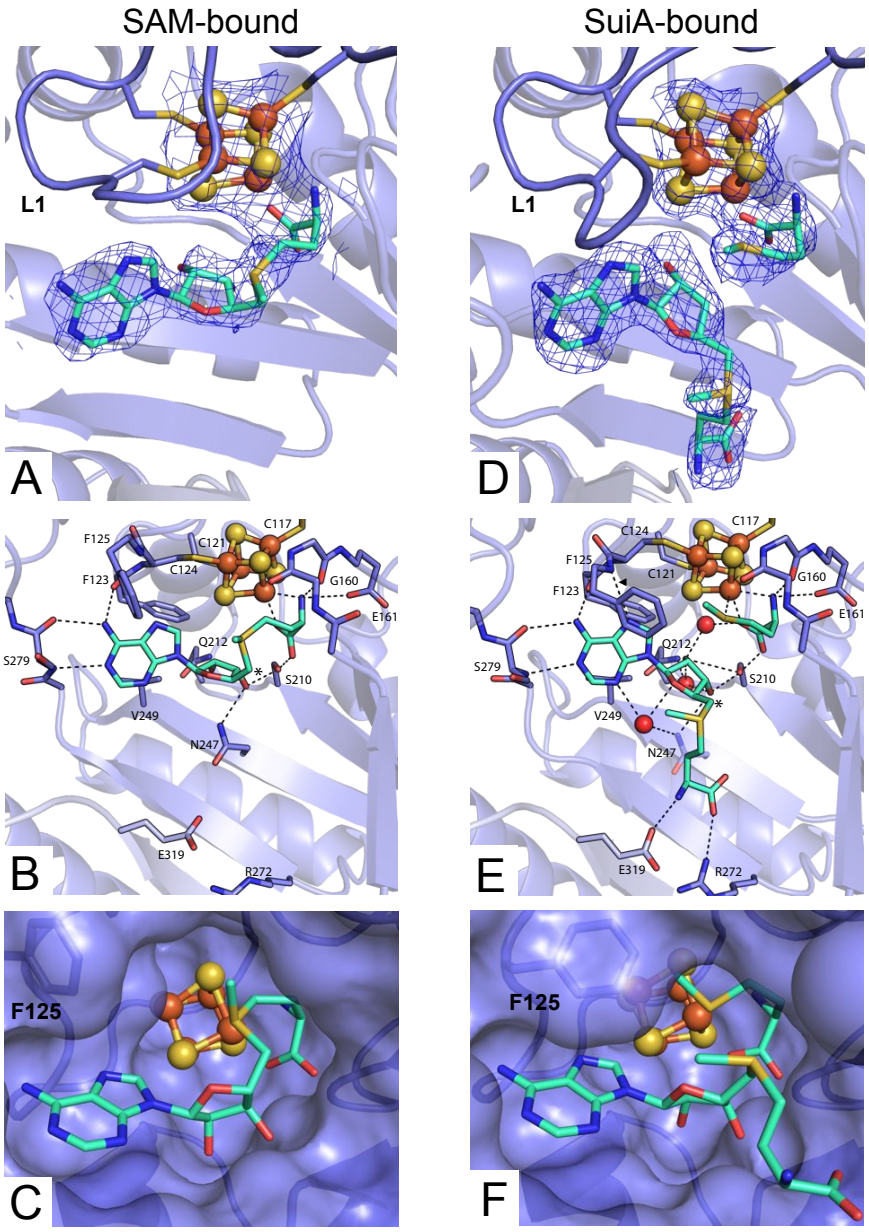

Figure S1. SAM binding and cleavage in the SuiB active site. (A) $2F_O$-F_C composite omit map contoured at 1.0 σ is consistent with an intact SAM bound to the catalytic [4Fe-4S] cluster (Fe – orange, S – yellow). (B) Although the cluster was initially reduced, excess SAM in the absence of reductant yields intact SAM bound in the active site. Hydrogen-bonding network and relevant residues from common radical SAM motifs are labeled. (C/F) Surface renderings of the active site for the SAM-bound and SuiA-bound structures, respectively, depict the formation of a hydrophobic pocket created by changes in loop 1, particularly the perpendicular stacking of F125 with the adenine moiety of SAM. (D) $2F_O$-F_C composite omit map contoured at 1.0 σ is consistent with methionine bound to the catalytic [4Fe-4S] cluster and an intact SAM in the 5'-dA pocket. (E) Post-cleavage hydrogen-bonding network and motifs that orient methionine and SAM (cyan) in the active site. Note the additional bond formed between F125 and 5'-dA as denoted by the arrowhead. The location of bond cleavage is marked with an asterisk.

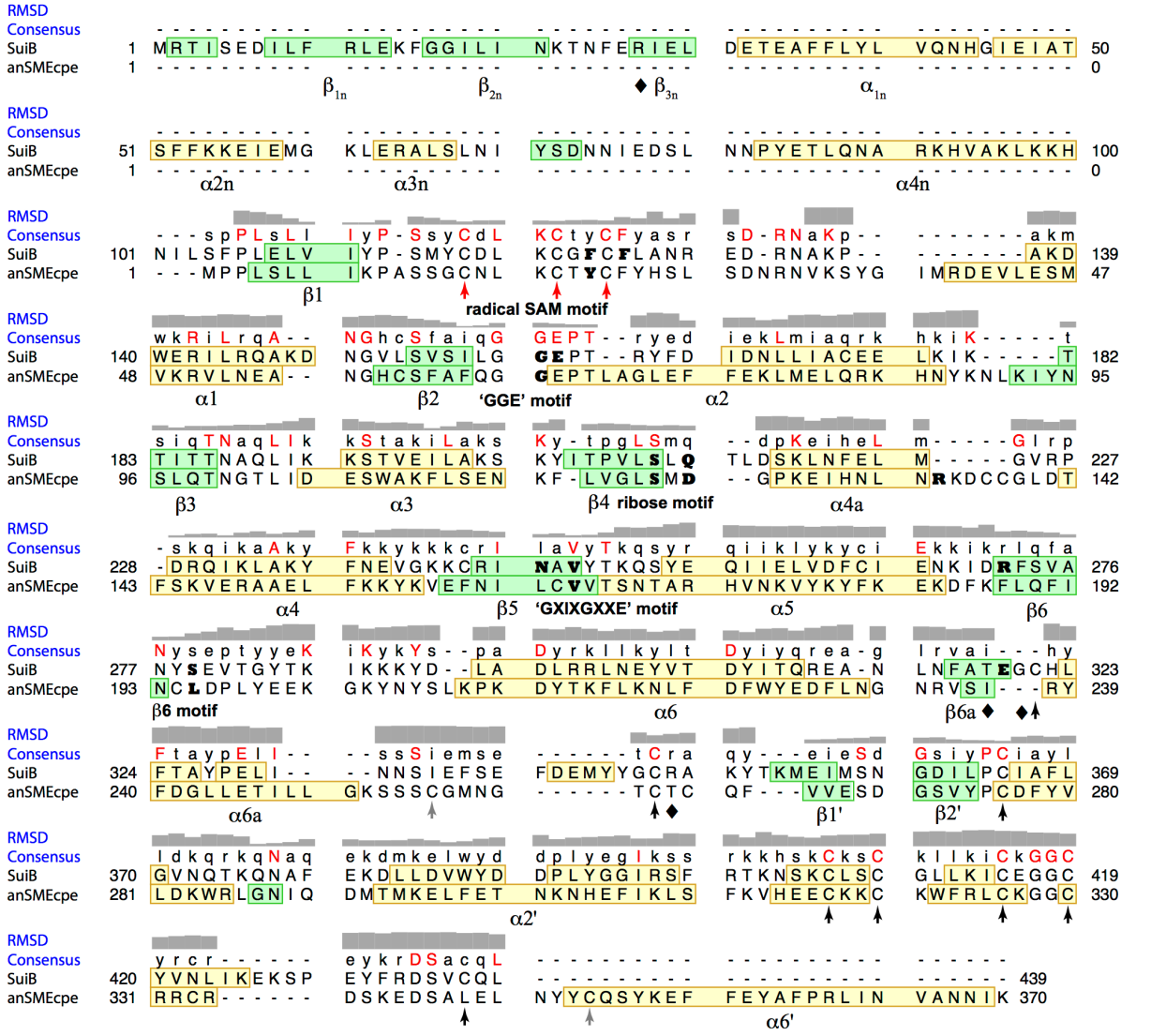

Figure S2. Sequence alignment of SuiB with anSMEcpe. A structure-based sequence alignment was generated using Chimera to yield an overall Cα rmsd of 4.82 Å for the aligned 309 residues. β-strands are shown in green and α-helices in yellow. Primary strands, helices and motifs are labeled below each feature. Secondary structure elements align well for the SAM and SPASM domains (res. 107–310/347–437 in SuiB and res. 3–234/261–348 in anSMEcpe respectively). A histogram, shown in grey, depicts the rmsd by residue, ranging from 0.36 Å to 28.84 Å. Residues that H-bond with SAM or methionine are shown in bold face, whereas black diamonds signify those that directly H-bond with the SuiA leader. Arrows denote Fe/S cluster ligating cysteines. Those corresponding to the SAM cluster are shown in red, the SuiB auxiliary clusters in black, and mismatched cysteines in anSMEcpe in grey.

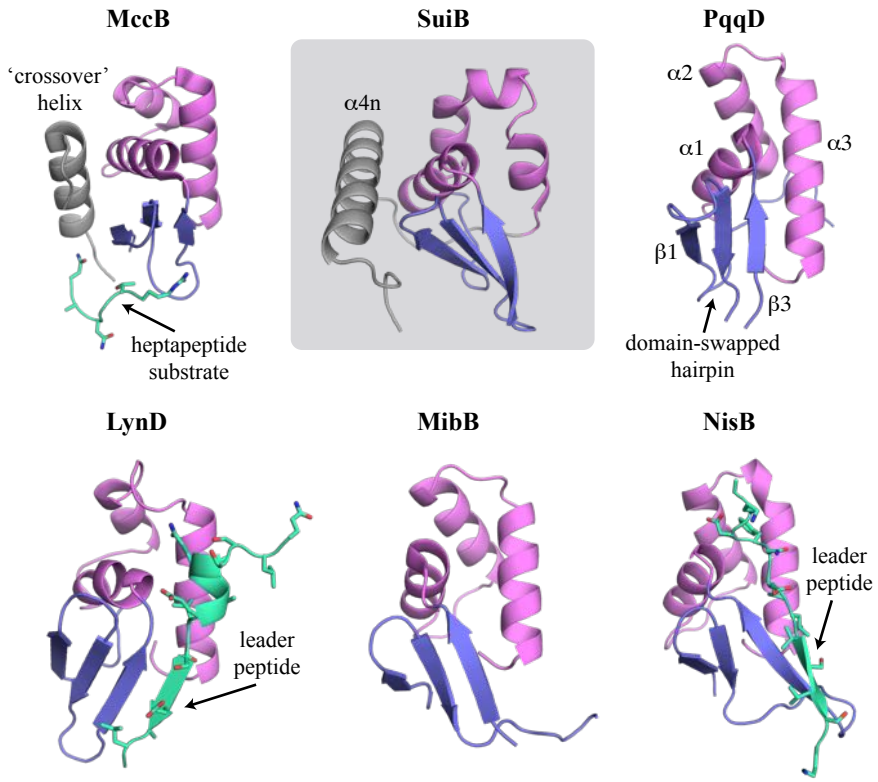

Figure S3. Comparison of the RRE domain in SuiB with those previously characterized by X-ray crystallography. LynD is a fused cyclodehydratase involved in cyanobactin biosynthesis (PDBID: 4V1T); MibB (PDBID: 5EHK) and NisB (PDBID: 4WD9) are lantibiotic dehydratases; MccB (PDBID: 3H9J) is an adenylase in the microcin C7 biosynthetic pathway; and PqqD (PDBID: 3G2B) is a peptide chaperone involved in the production of PQQ. The characteristic wHTH domain is depicted with purple strands and pink helices; precursor peptides are green. The ancillary helix, corresponding to $\alpha 4_n$ in SuiB, is shown in grey and domain-swapped elements of MccB and PqqD are labeled accordingly. The strands and helices in PqqD are labeled for clarity.

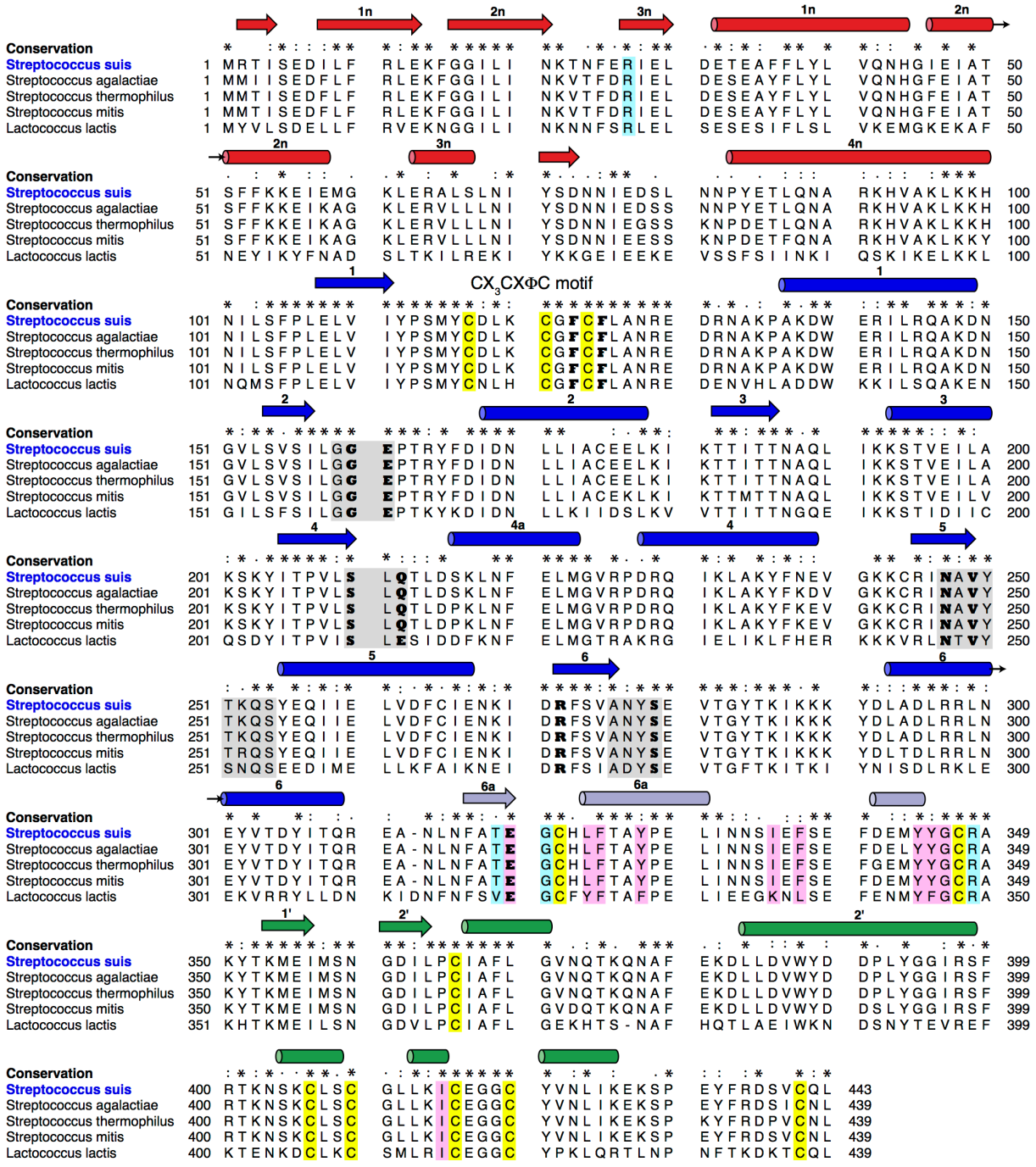

Figure S4. Sequence alignment of SuiB homologs. Consensus symbols are placed above each residue. An asterisk corresponds to a fully conserved position. A colon (period) indicates strong (weak) agreement between residue properties. Spaces display strong divergence. Strands and helices are shown as cartoons above each feature, with the primary elements labeled. Active site SAM-binding motifs are highlighted in grey, and Fe-ligating cysteines in yellow. Residues that H-bond with SAM or methionine in SuiB are shown in bold face. Hydrogen bonding partners for the leader portion of SuiA are likewise highlighted in blue; all other interacting residues are shown in pink.

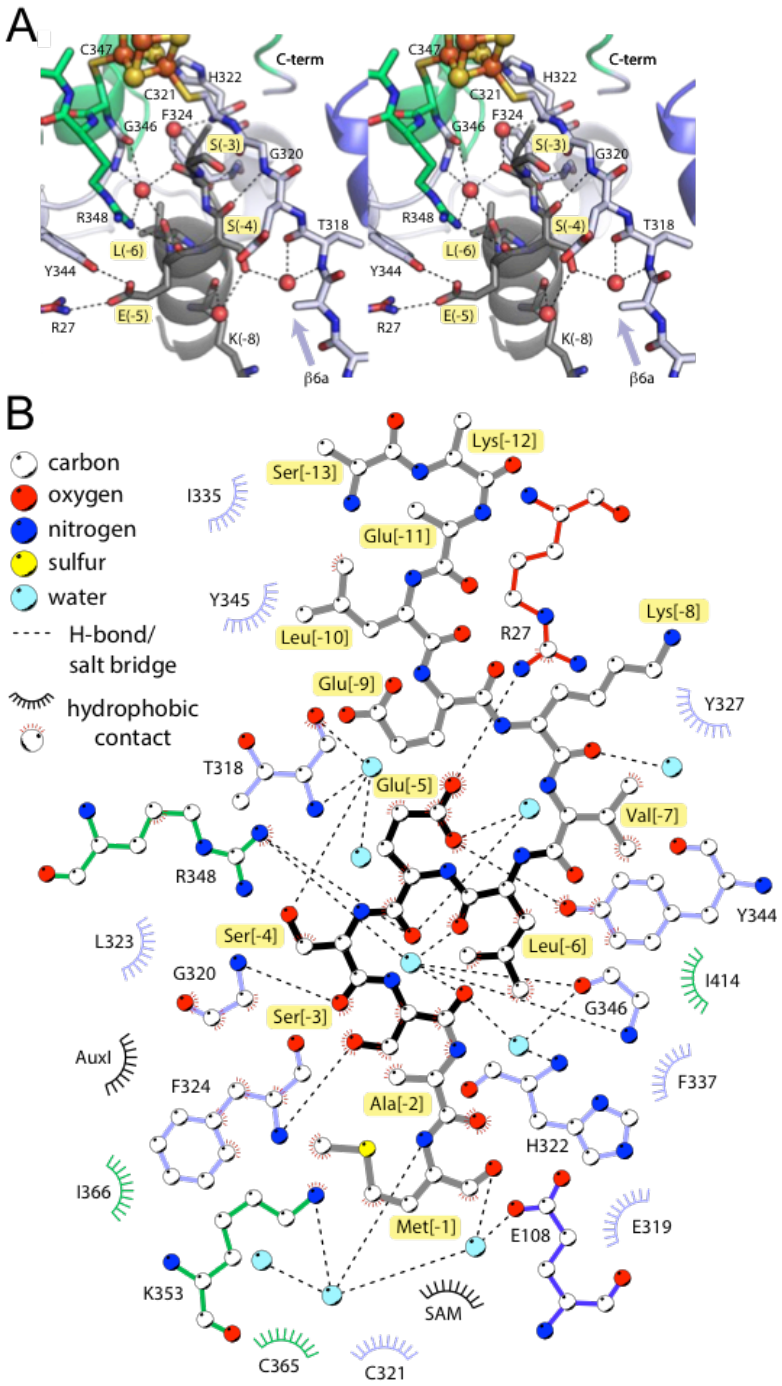

Figure S5. Leader peptide binding site of SuiB. (A) Stereo view depicting the H-bonding network of SuiA (dark grey) bound in the active site of SuiB. Residues from the bridging domain are shown in light blue, the SPASM in green and the N-terminal RRE domain in red. (B) 2-D protein/peptide interaction map. SuiA labels are highlighted in yellow. Hydrogen bonds are shown for distances less than 3.4 Å. As the electron density terminates immediately after SuiA-Met(-1), the direction of the side-chain and corresponding interactions are ambiguous. The displayed orientation was selected for feasibility of peptide continuation into the active site based on the Rosetta simulations.

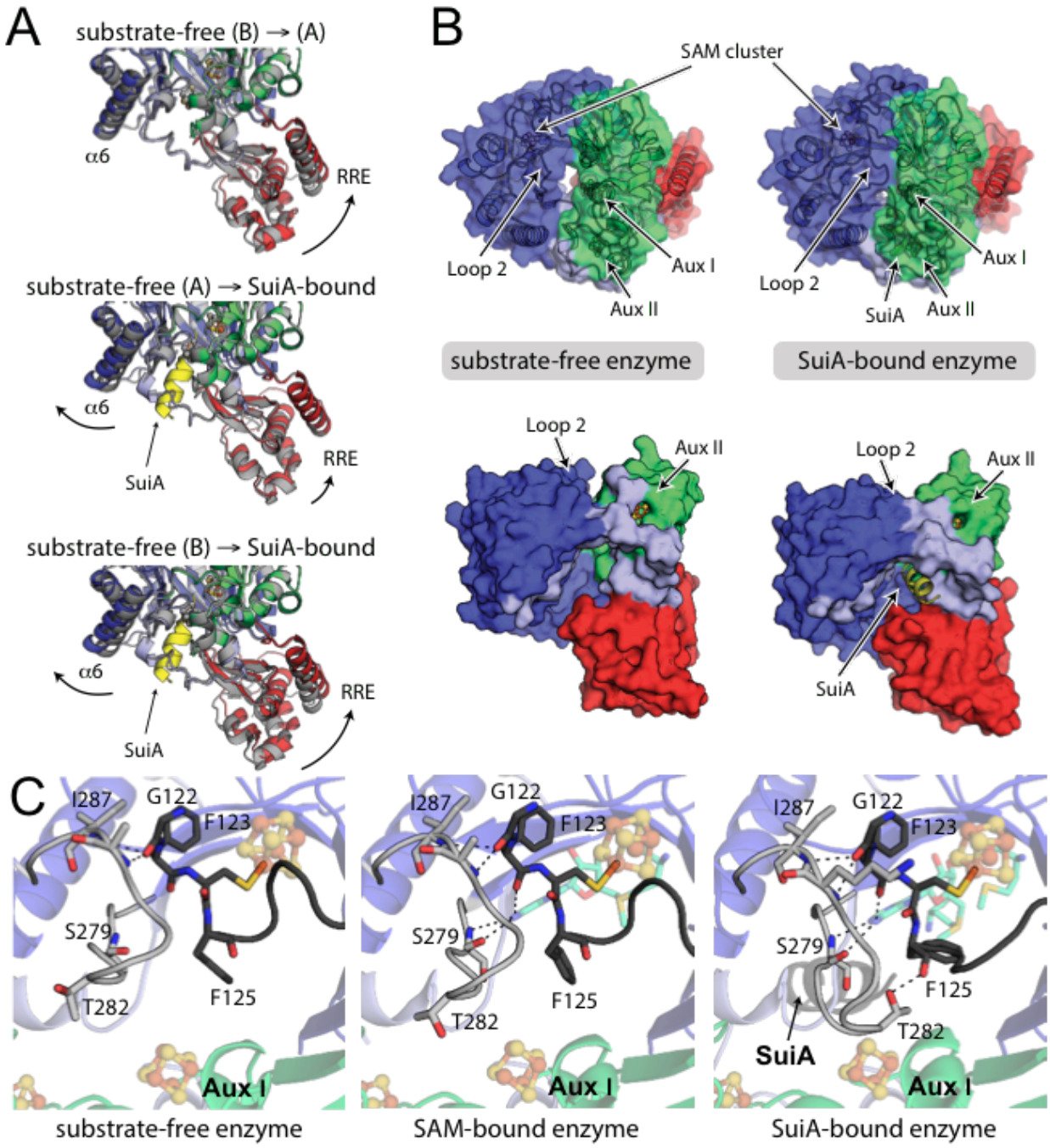

Figure S6. Conformational changes in SuiB upon binding of substrate SuiA. (A) Structural alignment of the substrate-free enzyme chains depict different conformations of the RRE domain and are thus compared independently with the SuiA–bound structure. The structure listed first is shown in grey. SuiA is shown in yellow for clarity. The two chains (A/B) in the asymmetric unit are denoted parenthetically. (B) Surface rendering depicting how the loop movements upon SuiA binding obstruct solvent access to Aux I, Aux II, and the active site. Clusters are shown in ball and stick representation (Fe – orange, S – yellow). (C) Hydrogen-bonding between loops (L1 – black, L2 – light grey) results in coordinated motions upon substrate binding. Upon binding, SAM mediates an additional hydrogen bond between the loops, as shown in Figure S1.

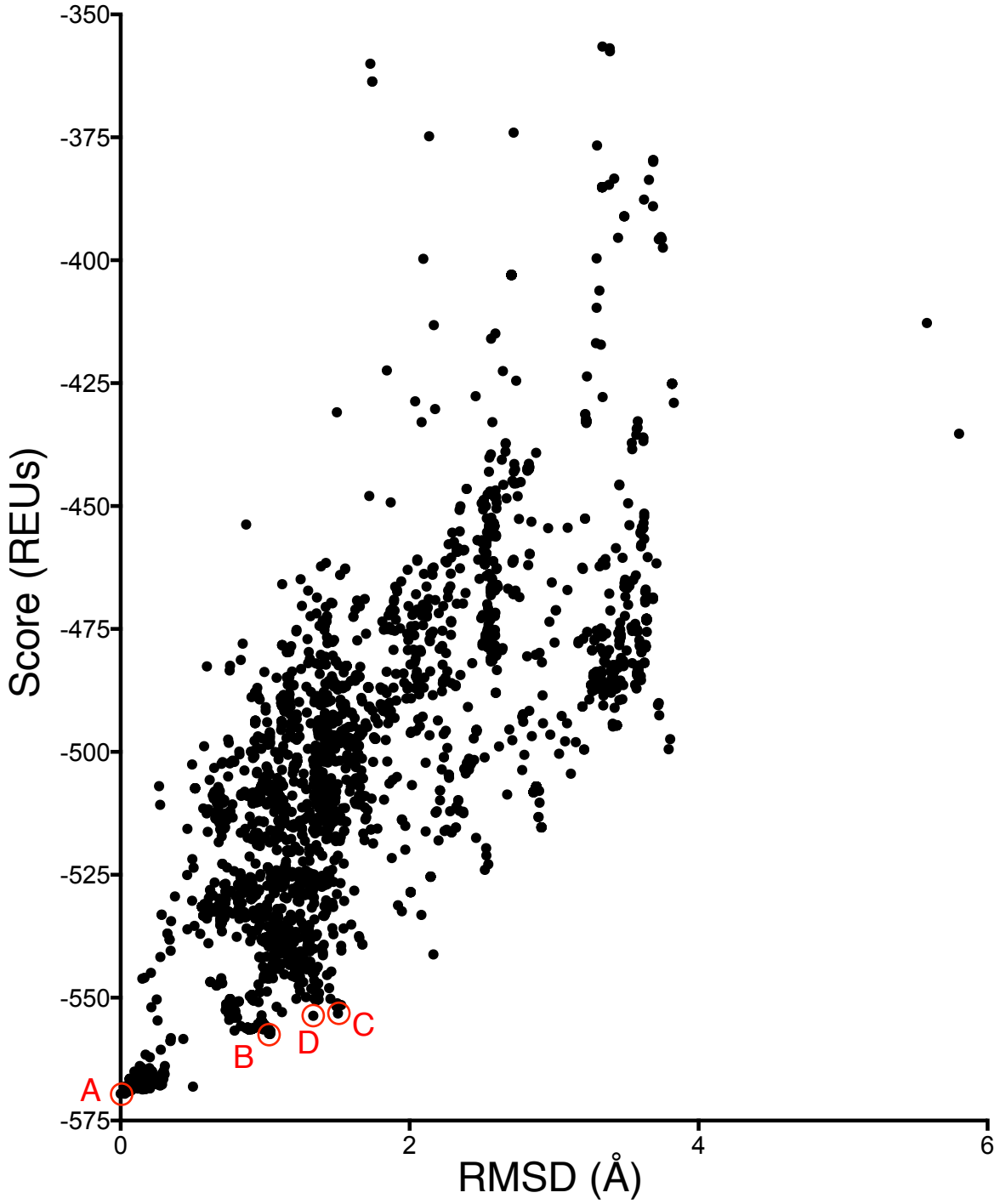

Figure S7. Energy landscape of the cyclized SuiA peptide in the SuiB active site. Score (Rosetta Energy Units) is calculated for the SuiA-SuiB complex for structural models at the end of FastRelax trajectories. RMSD is calculated with respect to the lowest energy models detected in the simulations. Conformations depicted in Fig. S8 are highlighted.

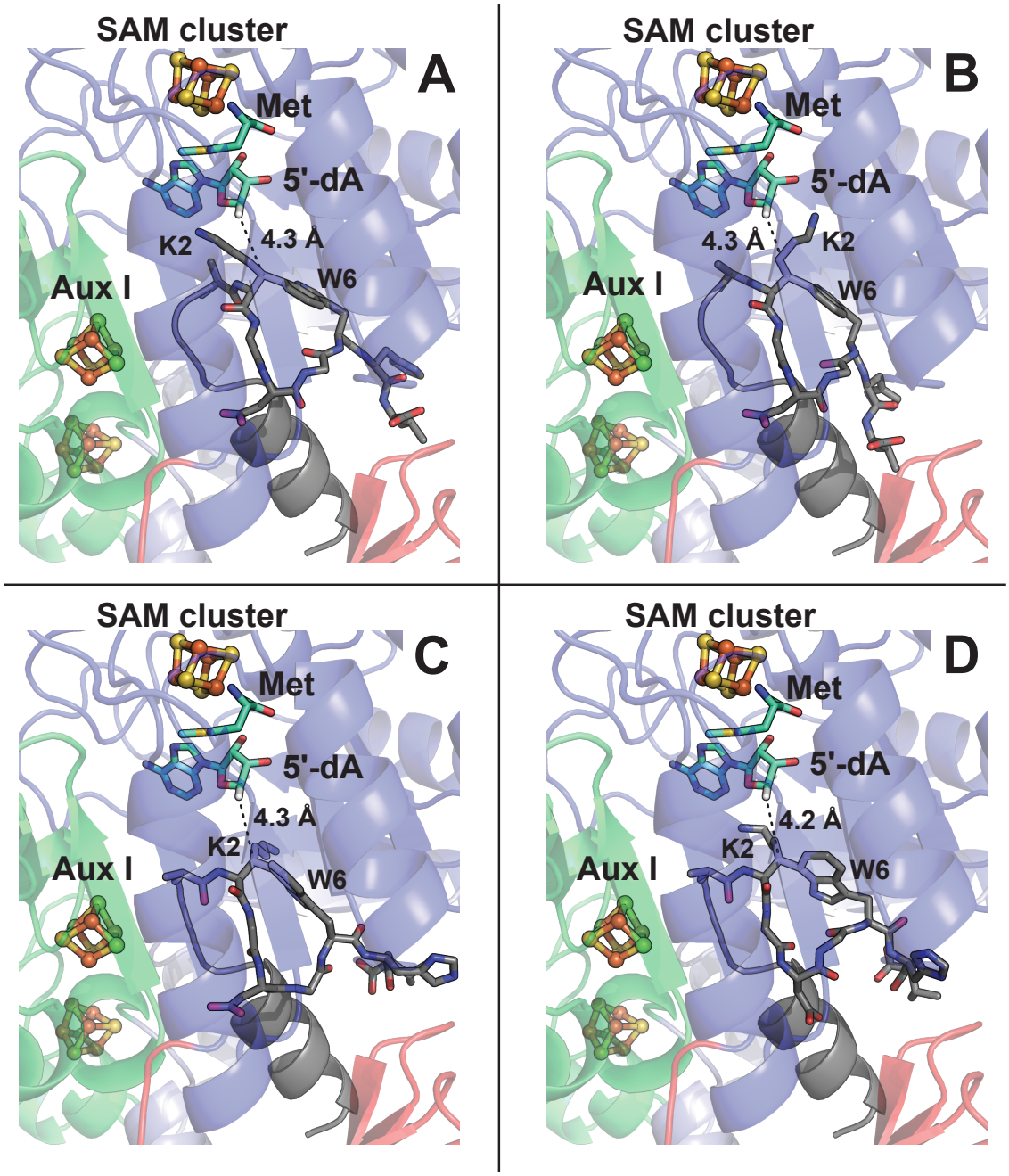

Figure S8. Rosetta simulations yielded four sets of distinct low energy conformations for the cyclized peptide when SAM was replaced with 5'-dA. Although very similar, the position of the lysine side-chain and C-terminal residues vary between groups A–C, while in group D the orientation of the indole side-chain is rotated. In all possible conformations, the C-terminus protrudes from the barrel due to space constraints. Hydrogen bonding between SuiA-Asp4 and Arg348 in groups A and B are in agreement with activity assays finding reduced turnover upon an Asp-to-Ala mutation (19).

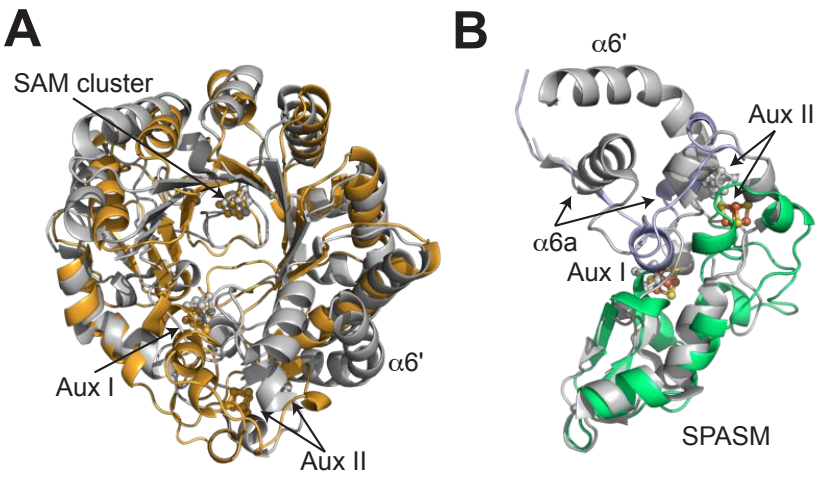

Figure S9. Structural comparison with anSMEcpe. (A) A sequence-independent alignment (RMSD = 3.1Å) of the anSMEcpe (PDB ID: 4K38 - grey) and SuiB (orange) barrels. The RRE domain was omitted for clarity. (B) Expanded view of the SPASM and bridging regions of SuiB (colored) and 4K38 (grey). Rearrangements of the linker region and α6' are required due to the binding position of SuiA within the barrel. The radical SAM domain is shown in blue, the linker in light blue, and the SPASM in green. Fe/S clusters are shown in ball and stick representation, where Fe is orange and S is yellow. The peptide substrate, SuiA, is also yellow and depicted in cartoon form.

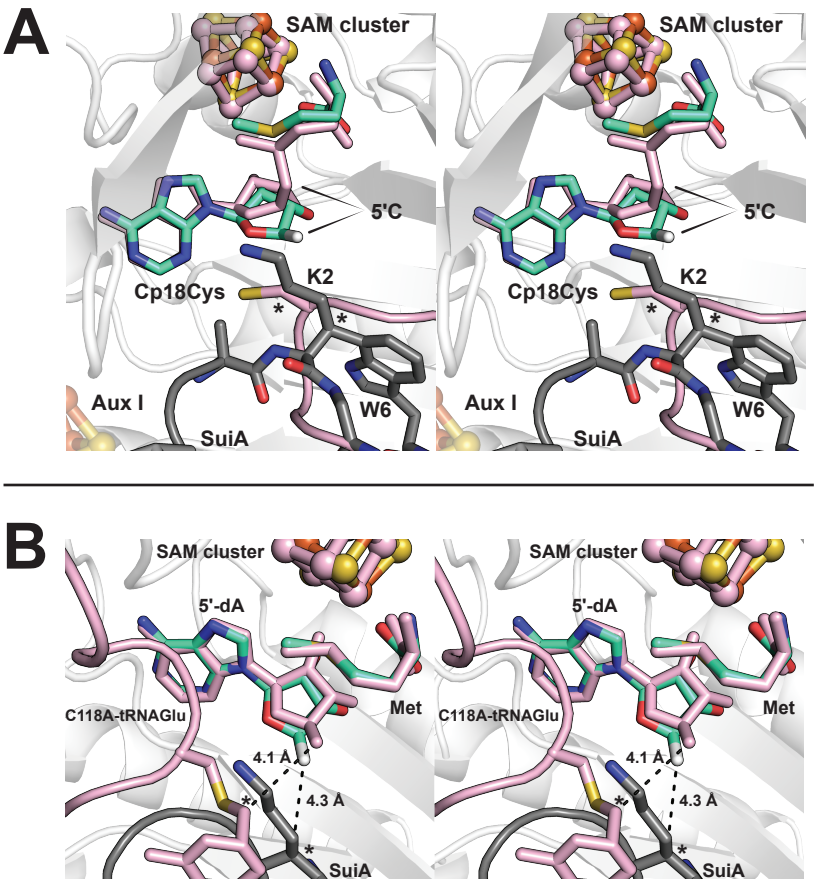

Figure S10. The simulated location of the Lys-to-Trp crosslink overlays well with the H-atom abstraction sites of (A) anSMEcpe (20) and (B) RlmN (21).

SI References

1. Broderick JB, Duffus BR, Duschene KS, Shepard EM (2014) Radical *S*-adenosylmethionine enzymes. *Chem Rev* 114(8):4229-4317.
2. Dowling DP, Vey JL, Croft AK, Drennan CL (2012) Structural diversity in the AdoMet radical enzyme superfamily. *BBA-Proteins Proteom* 1824(11):1178-1195.
3. Grell TAJ, Goldman PJ, Drennan CL (2015) SPASM and twitch domains in *S*-adenosylmethionine (SAM) radical enzymes. *J Biol Chem* 290(7):3964-3971.
4. Regni CA*, et al.* (2009) How the MccB bacterial ancestor of ubiquitin E1 initiates biosynthesis of the microcin C7 antibiotic. *Embo J* 28(13):1953-1964.
5. Schramma KR, Seyedsayamdost MR (2017) Lysine-tryptophan-crosslinked peptides produced by radical SAM enzymes in pathogenic streptococci. *ACS Chem Biol*.
6. Shisler KA, Broderick JB (2012) Emerging themes in radical SAM chemistry. *Curr Opin Struc Biol* 22(6):701-710.
7. Kabsch W (2010) XDS. *Acta Crystallogr D* 66(2):125-132.
8. Evans PR, Murshudov GN (2013) How good are my data and what is the resolution? *Acta Crystallogr D* 69(7):1204-1214.
9. Emsley P, Lohkamp B, Scott WG, Cowtan K (2010) Features and development of COOT. *Acta Crystallogr D* 66(4):486-501.
10. Adams PD*, et al.* (2010) PHENIX: A comprehensive python-based system for macromolecular structure solution. *Acta Crystallogr D* 66(2):213-221.
11. Chen VB*, et al.* (2010) MolProbity: All-atom structure validation for macromolecular crystallography. *Acta Crystallogr D* 66(1):12-21.
12. McCoy AJ*, et al.* (2007) Phaser crystallographic software. *J Appl Crystallogr* 40(4):658-674.
13. Zanghellini A*, et al.* (2006) New algorithms and an *in silico* benchmark for computational enzyme design. *Protein Sci* 15(12):2785-2794.
14. Stein A, Kortemme T (2013) Improvements to robotics-inspired conformational sampling in Rosetta. *PLOS ONE* 8(5):e63090.
15. Khatib F*, et al.* (2011) Algorithm discovery by protein folding game players. *P Natl Acad Sci USA* 108(47):18949-18953.
16. Richter F, Leaver-Fay A, Khare SD, Bjelic S, Baker D (2011) *De novo* enzyme design using Rosetta3. *PLOS ONE* 6(5):e19230.
17. Schramma KR, Bushin LB, Seyedsayamdost MR (2015) Structure and biosynthesis of a macrocyclic peptide containing an unprecedented lysine-to-tryptophan crosslink. *Nat Chem* 7(5):431-437.
18. Kuhlman B, Baker D (2000) Native protein sequences are close to optimal for their structures. *P Natl Acad Sci USA* 97(19):10383-10388.
19. Schramma KR, Seyedsayamdost MR (2017) Lysine-tryptophan-crosslinked peptides produced by radical SAM enzymes in pathogenic streptococci. *ACS Chem Biol*.
20. Goldman PJ*, et al.* (2013) X-ray structure of an AdoMet radical activase reveals an anaerobic solution for formylglycine posttranslational modification. *P Natl Acad Sci USA* 110(21):8519-8524.
21. Schwalm EL, Grove TL, Booker SJ, Boal AK (2016) Crystallographic capture of a radical *S*-adenosylmethionine enzyme in the act of modifying tRNA. *Science* 352(6283):309.